Chapter 15
Explanation of Metastasis by Homeostatic Inflammation

If inflammation caused by either non-self or self molecules can disseminate throughout the body and inflammatory sites actively allow entry of circulating tumor cells and assist their regrowth, then circulating tumor cells metastasize to the sites of inflammation. However, disrupted sites of homeostatic inflammation do not necessarily guarantee metastatic spread and subsequent regrowth.

Before explaining how tumor cells regrow in premetastatic organs with inflammatory properties, there is a fundamental issue of whether or not extrinsic factor-induced inflammation, systemic or localized, facilitates metastasis in the inflammatory lesion.

15.1 Local Stimuli

15.1.1 Irradiation at Primary Sites

Although a rare case of metastasis of lung cancer to a minor traumatic lesion has been reported, mechanical injury seldom allows metastatic growth of tumor, otherwise surgeons lose their job.

Radiation to the thorax or pelvis of tumor-non-bearing normal mice increased serum TGFβ1 levels by twofold for at least 7 days [1]. MMTV/PyMT transgenic model of metastatic mammary tumor showed that thoracic irradiation at 10 Gy by shielding other portions of the body enhanced lung surface metastasis by threefold at 2 weeks after irradiation. This took place in a manner dependent on TGFβ1 in the tumor cells, because conditional depletion of TGFβRII using Cre/Lox technology reversed the effect. TGFβ1, which is induced by irradiation in a tumor-independent manner, is thought to facilitate directly the survival of the tumor cells. In this case, the lungs were not irradiated to cause inflammation but tumor burden by itself

Y. Maru, *Inflammation and Metastasis*, DOI 10.1007/978-4-431-56024-1_15

induce premetastatic conditions in the lungs and irradiation-induced serum TGFβ1 activates CTC to reach the lungs.

UV-irradiated epidermal keratinocytes secrete HMGB1, which activates TLR4 to recruit neutrophils in the irradiated skin in which $CD11b^+$ $Ly6C^+$ $Ly6G^+$ cells dominate [2]. In transgenic mouse model of melanoma that overexpressed HGF and an oncogenic CDK4, repeatedly irradiated mice by UV for 6 weeks exhibited some melanoma cells expanding along the endothelial cells, often observed in human melanoma. This angiotropism enhanced lung metastasis, both of which were abrogated in KO mice of either TLR4 or MyD88. Also in this experiment, lungs were not treated by UV, but the generated melanoma by UV prepared premetastatic soil in the lungs.

In both experiments, irradiation of tumor induced host cell responses, which provide favorable conditions for tumor cells to achieve metastasis, such as potentials to intravasate and survive.

15.1.2 Hepatitis

Meta-analysis of 4049 patients who suffered from chronic liver diseases, including fatty liver, chronic hepatitis virus B or C infection, and cirrhosis, revealed significantly lower rates of liver metastasis in colorectal cancer (CRC) [3]. Readers should remember that the organ first encountered by circulating tumor cells from the primary tumor is liver by CRC, lungs by any tumors that do not drain into the portal vein, and any organs by lung cancer. A more focused analysis of chronic viral hepatitis (CVH) B and C, liver metastasis took place in 2.86% (2 of 70 cases) compared with 16.9% (48 of 284) in non-CVH. In C57BL/6 mice with cirrhosis, which was induced by carbon tetrachloride gastrogavage for 2 months, B16F1 melanoma cell injection via the portal vein caused seven- to ninefold increase in frequency of tumor in the liver by histological analysis in cirrhosis over the untreated group [4]. No surface metastatic nodules were found in the lungs. Intravital kinetic analysis showed that the tumor cell movement was slower in the cirrhotic group. Given the presence of regeneration, fiber generation and inflammatory cells in both clinical autopsy and experimental mouse settings, I assume that inflammatory nature in the liver and its matching with tumor cell property may make a difference.

15.1.3 Bacteria or Lipopolysaccharide

Treatment of B16 melanoma cells with lipopolysaccharide (LPS) or lipid A at 1 μg/ml each for 48 h, which induced CCL2 expression, followed by extensive washing and subcutaneous implantation, reduced the tumor growth compared with untreated B16 cells in both wild-type and TLR4-KO mice. However, LPS promotes tumor

cell migration in vivo [5]. Supportive evidence has been provided by experiments in which direct intratracheal administration of either *Escherichia coli* or LPS before injection of tumor cells, such as B16F10 melanoma or RM-9 cells, through the tail vein enhanced lung metastasis at 14 days after tumor challenge [6]. Tumor cell injection at any time points earlier than 6 h, but not later than 3 days, of LPS was effective for the enhancement. BAL fluid 6 h after LPS had increased amounts of IL-6, G-CSF, KC, SDF-1, and extracellular ubiquitin. The major chemokine receptor of neutrophils in acute lung inflammation is CXCR2, which is activated by MIP-2 and KC (remember that KC is a rodent version of IL-8 in humans). As with TLR4, CXCR2 is expressed in both blood and non-blood cells, both of which contribute to neutrophil accumulation and pulmonary permeability in the lungs. Both ubiquitin and SFD-1 are known to bind CXCR4, and CXCR4 inhibitor AMD3100 blocked the enhancement of metastasis. The reasonable but important point is that they found no metastasis in the extrapulmonary organs. In our laboratory, LPS administration through a catheter only to the left bronchus with microspheres to make sure of the stimulation sites induced vascular permeability at 48 h and accumulation of intravenously injected labeled tumor cells in the left but not right lung. Therefore, a local TLR4 activation of a given pulmonary segment causes a limited inflammatory space to which tumor cells are allowed to metastasize. If the lung TLR4 is activated by an endocrine manner, the whole lungs should be transformed to be premetastatic soil.

15.2 Systemic Stimuli

15.2.1 Arthritis

MMTV-PyV MT mice display no primary mammary tumor at 9 weeks, but during the period of 18–26 weeks tumors with spontaneous metastasis appear. Rheumatoid arthritis mouse model by type II collagen injection was performed intradermally at 9 weeks of MMTV-PyMT mice to induce arthritis in 11–13 weeks of tumor development [7]. The combined systems at early developmental stages of mammary tumor are assumed to see the systemic inflammatory effect at the premetastatic phase. Bone metastasis took place only in the arthritis mice, and more than twofold increase in lung metastasis was observed in the same group. The arthritis induction caused leukocyte infiltration in the lungs, which was enhanced by roughly fourfold in the background of mammary tumor. Elevation of factors in the lungs and circulation was detected, including IL-17, IL-6, and PGE2. Anti-IL-17 antibody and COX-2 inhibitor both reduced the metastasis. The same group demonstrated that arthritis induced mast cell recruitment in the lungs in a tumor-independent manner, but tumor cell engagement enhanced the mast cell activation underpinning the enhanced metastasis [8]. Anti-c-Kit antibody also was effective to

reduce metastasis. Importantly, the detailed experiments tell us that premetastatic soil can be cultivated by inflammation of other organs.

15.2.2 Allergy

The experimental method to induce allergic inflammation in lungs has been established. Intraperitoneal injections of chicken ovalbumin (OVA) followed by repeated aerosol challenges can provoke mucus accumulation in respiratory tracts and airway hyperresponsiveness, serving as an asthma model [9]. The James J. Lee group has demonstrated that $CD4^+$ T-cell-dependent recruitment of eosinophils in both bronchoalveolar lavage fluid (BAL) and interstitial peribronchial and perivascular areas are required for the asthmatic phenotypes by engineering eosinophil-lacking PHIL mice in which expression of cytocidal diphtheria toxin is congenitally driven by the eosinophil peroxidase gene promoter. Gαi2-dependent CCR3 signaling promotes transendothelial migration of eosinophil [10].

When B16F10 melanoma cells were injected through the tail veil after aerosol challenges, numbers of metastatic foci on the pulmonary surface were increased by threefold [11]. T cell depletion by anti-CD4 antibody (GK1.5), corticosteroid inhalation and Gαi2-KO condition, but not the PHIL background, abrogated the enhanced metastasis. Therefore, it is not eosinophils by themselves but $CD4^+$ T-cell-dependent soil preparation to allow transendothelial migration of cells that appears to play a critical role for allergy-facilitated lung metastasis. The same group provided data of 176 breast cancer patients with lung metastasis. Approximately 13% suffered from asthma but with no corticosteroid treatment, which is about twice the frequency of asthma in a random population of American females.

15.3 Disruption of Local Homeostasis

CC10, alternatively called club cell secretory protein (CCSP) or uteroglobin (UG), is secreted by club cells in a steroid-inducible manner. CC10-KO mice are susceptible to LPS inhalation with increased leukocytes in BAL 24 h after LPS [12]. The concentration gradient of S100A8 was detected in the lungs down to blood in CC10-KO mice [13]. CC10-KO enhanced lung metastasis after injection of B16F10 melanoma cells through the tail vein. Although S100A8 was not expressed in B16F10 cells, they expressed RAGE whose ligand includes AGE and S100A8/S100A9. An anti-RAGE siRNA-mediated knockdown of RAGE in B16F10 prior to the tail veil injection suppressed lung metastasis. I assume that CC10-KO lungs are already cultivated by constant assaults of bacteria with LPS for the expression of S100A8 and S100A9 before tumor cell injection.

15.4 Disruption of Systemic Homeostasis

15.4.1 VEGFR2-CN-NFATc Homeostatic Feedback by DSCR-1

The calcineurin-NF-ATc pathway has been known as located downstream of antigen-presenting cell engagement to T cells but also is activated individually by the VEGF-VEGFR2 and thrombin-PAR-1 systems [14]. Both exert vascular permeability as I stated earlier. From cDNA microarray experiments of HUVEC stimulated by VEGF and thrombin, Down syndrome critical region-1 (DSCR-1, also called calcipressin 1, MCIP-1, and adapt 78) was found dramatically induced by 22.3-fold and 17.7-fold, respectively at 1 h [15]. It turned out that DSCR-1 inhibited nuclear localization of NF-ATc in HUVEC, i.e., inhibited calcineurin activity by direct interaction. The NF-ATc-mediated transcription induces expression of cytokines, such as IL-6, but simultaneous induction of the inhibitory molecule DSCR-1 forms a negative feedback loop to brake hyperactivation of the cytokine storm.

The expression of ICAM-1, E-selectin, and VCAM-1 were negatively affected by more than 50% in thrombin-stimulated HUVEC infected with DSCR-1 adenovirus [16]. Not only the mRNA expression level but also number of genes was down-regulated by DSCR-1. The same author stated that 52 of 172 thrombin-activated genes in HUVEC were down-regulated by DSCR-1 overexpression. Given that both VEGFR2 and PAR-1 provoke inflammation, the autoinhibitory mechanism serves to avoid an overshoot and maintain the oscillating physiological levels of calcineurin-NF-ATc activity. Therefore, this also can be called homeostatic inflammation.

Adenovirus-mediated gene transfer of DSCR-1 in B16 melanoma xenograft at approximately 50 mm^3 tumor size, in which angiogenesis was actively taking place, inhibited the tumor growth. However, syngrafts of murine renal carcinoma (RENCA) and colon cancer (MC26) in DSCR-1^{-}KO mice displayed diminished tumor growth with significant reduction in $SMA^{+}CD31^{+}$ vessels [17]. Mechanistically, constitutive activation of calcineurin not only induced precocious NF-ATc nuclear localization in a cyclosporine-inhibitable manner but also dephosphorylated BAD to activate the apoptosis pathway in endothelial cells. Cerebral hemorrhage was detected in 15% of DSCR-1-KO at embryonic days 10 and 12 (E10 and E12).

Those experiments tell us important logics in homeostasis. There are several modes in negative feedback by molecules downstream, including catalytic inhibition of the molecule upstream by keeping the cells alive and cancellation of the biological outcome, such as growth, by eliminating the cells by apoptosis. It depends on the developmental stage of embryos and tumors. Another example of endothelial homeostasis is VEGF. Anti-VEGF antibody also resulted in side effects, such as brain hemorrhage [18]. VEGF-KO mice are embryonic lethal [19].

In ectopic syngraft model with eGFP-labeled B16F10 melanoma cells, premetastatic lungs were assumed by 12 days after subcutaneous implantation [20]. They found fibrinogen-fibrin deposit generated by vascular instability that is caused by expression of angiopoietin 2 (Ang2), MMP3, and MMP10. They could hardly detect up-regulation of VEGF in the lungs and claimed that both TGFβ and TNFα were responsible for up-regulation of those molecules, siRNA-mediated knockdown of which resulted in suppressed infiltration of both myeloid cells and tumor cells. Ang2 is usually expressed in vascular remodeling sites in which vessels are more plastic with loosened endothelial junctions. Our experiments showed that blocking TGFβ and TNFα individually suppressed up-regulation of S100A8 and S100A9 in premetastatic lungs of tumor-bearing mice.

When B16F10 melanoma cells were injected via the tail vein to Dscr1-lacZ mice, in which LacZ expression was engineered to manifest the calcineurin-NF-ATc activity, tyrosinase mRNAs were not detected until day 7 after tumor cell injection. Because it could be detected as early as days 3–5 before tumor cell arrival, they assumed the period as the premetastatic period. Interestingly, B16F10 injection in DSCR-1-KO mice significantly enhanced lung metastasis as judged by day 10. Orthotopic RENCA tumor model and LLC footpad model also aggravated lung metastasis in DSCR-1-KO mice, while growth of the primary tumor was suppressed as just described. The difference between the primary sites and metastatic lungs turned out to be Ang2 expression in the lungs without endothelial apoptosis. Up-regulation of both VEGF and activated VEGFR2 was recognized in the tumor-injected DSCR-1-KO mice.

15.4.2 Inflammation in Vessels

I have repeatedly stated the importance of vascular permeability in inflammation (Fig. 15.1; see also Chap. 14). What will happen when endothelial cells are systemically injured? It has been intensively studied from the standpoint of hypertension and vascular tone. Vascular tone is how much a vessel is constricted compared with maximum dilatation with largest lumen diameters. For example, angiotensin II (ATII) (amino acids 1–8) increases vascular tone, while by atrial natriuretic peptide (ANP) decreases it.

An early study in 1972 showed that ATII induced vascular permeability with interstitial edema in rabbit aorta and dermis in 30 min with Evans Blue as an indicator, which was accompanied by widening of inter-endothelial gaps by endothelial contraction [21]. ATII-stimulated vessels secrete PGE, which further increases permeability and induces vasodilatation.

ATII infusion for 14 days in mice displayed hypertension, reduced acetylcholine-mediated relaxation, increased maximum response to norepinephrine, hypertrophic remodeling with prominent macrophage infiltration, Nox2 up-regulation, and NFκB activation [22]. Those are attenuated in Op/Op mice

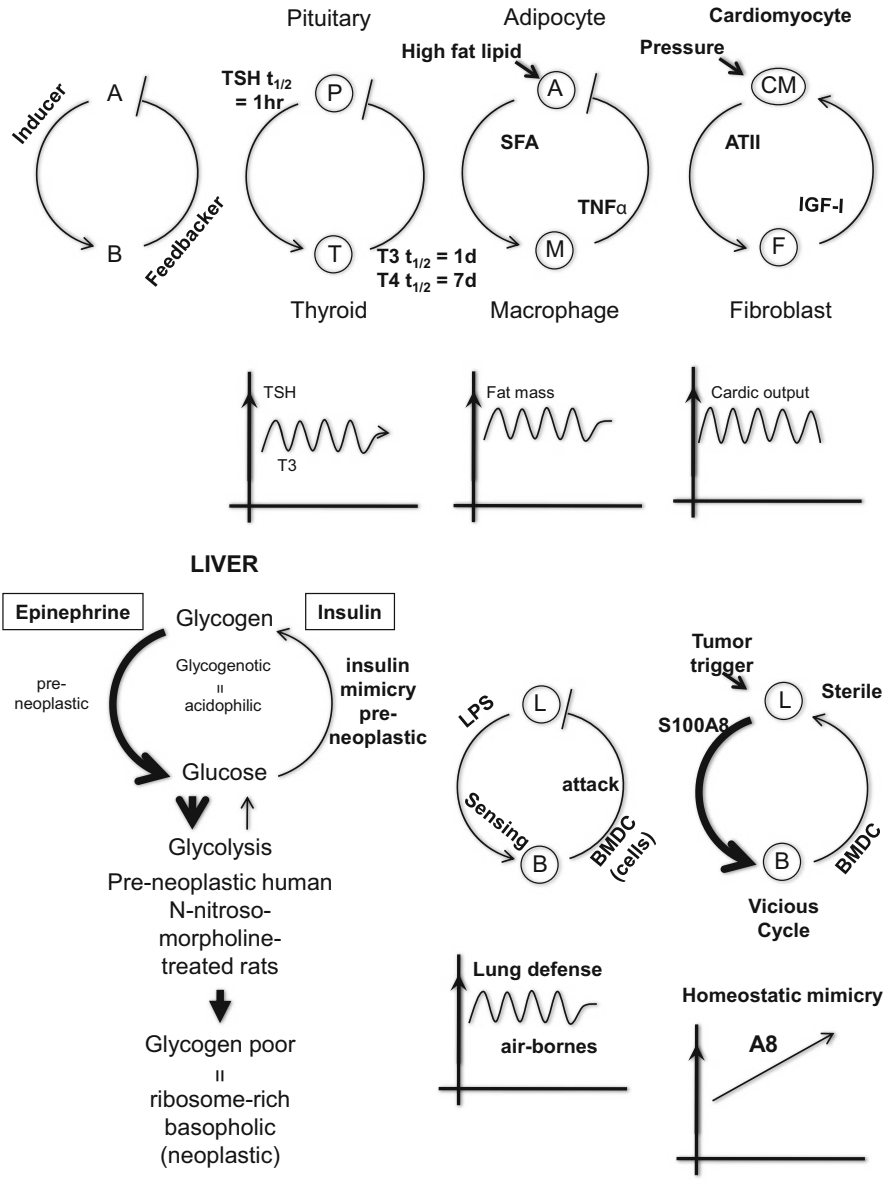

Fig. 15.1 Homeostatic mimicry

that are deficient in M-CSF showing monocytopenia and macrophage deficiency. In the same vessel injury model under the background of LDL-R-KO to induce hypercholesterolemia, development of atherosclerosis and aortic aneurysm was reduced by whole-body genetic deletion of ATII type 1a receptor (AT1a) [23]. The ATII-induced inflammation in vessels is accompanied by leukocyte

migration through activation of endothelial AT1a of both endothelial cells and vascular smooth muscle cells (VSMC) and the stimulated VSMC secretes the potent permeability factor VEGF and stimulated endothelial cells secrete chemokines, including CCL2, RANTES, MIP-1α, and IP-10 [24]. Conversely, VEGF-induced vascular permeability is blocked by pharmacological inhibitors against ATII receptor. Here the vasoconstrictor induces inflammation-mediated increase of vascular tone.

In the renin-angiotensin system (RAS), angiotensinogen is processed to ATI (amino acids 1–10) by renin, which is further cleaved by ACE to ATII. Both ATI and ATII are inactivated by ACE2, a homolog of ACE, to AT (amino acids 1–9) and AT (amino acids 1–7), respectively. ACE2 negatively regulates RAS. Although the baseline levels of pulmonary ATII were not changed in ACE2-KO mice, lung injury by acid (see Chap. 6) significantly augmented its levels in ACE2-KO mice, which was accompanied by severe lung edema due to enhanced pulmonary vascular permeability as judged by Evans Blue but not to changes in pulmonary perfusion pressures. The high permeability was abrogated in AT1a-KO mice or pharmacological inhibitor for AT1 receptor [25, 26].

When B16F1 melanoma cells were intravenously injected, lung metastasis was reduced in AT1a-KO mice [27, 28]. Conversely, oral administration of ATII enhanced the metastasis. The authors showed an engagement between B16F1 cells with ATII-induced expression of P-selectin glycoprotein ligand-1 (PSGL-1) and platelets expressing P-selectin prompted VEGF release from the platelets. It is likely that ATII not only stimulates pulmonary endothelial cells to induce inflammation but also B16F1 cells to induce PSGL-1 expression to facilitate the engagement. The important point is that AT1a-expressing tumor cells may reach the premetastatic lungs and wait for an angiogenic switch, which could be mediated by ATII that plays a homeostatic role in the lung microenvironment. Macrophages also express ACE to generate ATII [29].

TNFα can induce vascular permeability as stated before. Transgenic mice of TNFα exhibited lung emphysema and severe pulmonary hypertension (PH) with vascular remodeling, such as interstitial thickening and perivascular fibrosis [30]. Because nitric oxide (NO) at 25 ppm failed to restore the right ventricular pressure, PH was not due to sustained vasoconstriction. In a skeletal muscle, TNFα infusion induced increased capillary permeability but only a minor effect on vascular tone [31]. The vascular permeability factor eventually increases vascular tone after sustained TNFα-induced inflammation.

Knockout mice of NPR-A, one of the receptors for ANP, displayed systemic hypertension [32]. However, LPS-induced vascular permeability in the lungs could be partially attenuated by ANP infusion even in NPR-A-KO mice, suggesting that ANP also may use other receptors, such as NPR-C, for pulmonary barrier protection [33]. Therefore, ANP not only decreases vascular permeability but also decreases vascular tone, i.e., causes vasodilatation. Lung metastasis induced by intravenous infusion of B16 melanoma cells after pretreatment with LPS was reduced by 75% by ANP infusion prior to the tumor cell challenge [34]. Pretreatment with ATII also

enhanced lung metastasis, which was inhibited by candesartan, an AII receptor blocker [35].

15.4.3 AA Metabolites

Now I state on arachidonic acid (AA) metabolites in vascular tone. In endothelial cells, AA is metabolized to (1) PGI2 by cyclooxygenase (COX), (2) 12- or 15-HETE (hydroxyeicosatetraenoic acid) by lipoxygenase (LOX) and 11, 12- or 14, 15-EET (epoxyeicosatrienoic acid) by cytochrome P450 epoxygenases like CYP2C8 and CYP2J2. The EETs are subsequently metabolized into DHET (dihydroxyeicosatrienoic acid) with reduced biopotency by soluble epoxide hydrolase (sEH) (see Fig. 1.4 in Chap. 1).

Endothelial cells decrease their vascular tone individually by PGI2, NO, and endothelium-derived hyperpolarizing factor (EDHF), such as EET [36]. Independence of those factors can be understood by non-NO and non-PGI2-mediated relaxation even in the presence of pharmacological inhibitors against NOS and COX. To complicate the circumstances, many factors participate in their release. For example, histamine induces release of PGI2 and EET. EET also is released by acetylcholine and bradykinin. EET opens Ca2+-activated K-channel and hyperpolarizes the membrane.

Syngeneic xenograft tumor models, including B16F10 melanoma, T241 fibrosarcoma, and LLC in the background of Tie2 promoter-driven CYP2C8, CYP2J2 transgenic (tg) and sEH-KO mice to achieve high levels of EET in endothelial cells exhibited dramatic increase in the tumor growth with enhanced tumor angiogenesis as judged by CD31-positive cells [37]. Transgenic mice of Tie2-sEH gave opposite effects. An enhanced corneal tumor angiogenesis was observed after systemic administration of 14,15-EET. In addition, stimulation of metastasis after removal of LLC primary tumor was further augmented in the background of those EET-high mice. I underline that they observed that the affected metastatic organs were multiple, including lymph nodes, liver, and lungs even without removal of the primary tumor. The EET-high tumor-bearing mice after tumor removal showed high levels of plasma VEGF and the resected tumor expressed high VEGF mRNAs. Most importantly and intriguingly, the authors performed parabiosis experiments to share circulation between, for example, a tumor-bearing Tie2-sEH-KO mouse as a donor with high EET and a Tie2-sEH-tg mouse as a recipient with low EET. This parabiosis gave enhanced tumor growth but the opposite condition, i.e., tumor in EET-low mice failed to enhance it. The shared high levels of EET were not sufficient to enhance tumor growth and endothelial EET levels were critical. It also was the case in metastasis. A tumor-bearing Tie2-CYP2C8-tg mouse with high EET failed to enhance metastasis in the recipient Tie2-sEH-tg mouse, demonstrating that endothelial EET levels control the metastatic microenvironment.

EET is produced in endothelial cells and therefore it appears to circulate and act on endothelial cells of the whole body. However, even in conditions where EET

could work in an endocrine manner, local actions in each endothelial cells appear to control its bioactivity. Both transgenic and KO engineering just provides artificial circumstances in which the endothelial EET simultaneously affects all endothelial cells of the whole body.

15.5 Obesity

Benign fat tumors are functionally malignant (Fig. 15.1; see also Chap. 14). A similarity can be recognized between cancer and adipose tissue. CCR2- and TLR4-promoted myeloid cells are mobilized in the primary tumor sites, premetastatic sites, and adipose tissues in obesity. The accumulated macrophages facilitate the tumor proliferation in the primary sites and hypertrophy of the adipocytes. Therefore, adipose tissues can be assumed to be benign tumors, because adipocytes do not make metastatic progression to different locations of adipose tissues nor circulating bone marrow-derived cells differentiate into adipocytes. Analyses of adipose tissue of mice that underwent BMT with GFP^+ bone marrow revealed that there were no GFP^+ cells that also were positive perilipin, an adipocyte marker [38].

15.6 Homeostatic Mimicry in Cancer

15.6.1 Insulin Mimicry in Preneoplastic Foci in Liver

A situation in which tumor cells utilize host homeostatic systems was proposed by Peter Bannasch in 1997 [39] (Fig. 15.1). The glycogen storage system in liver is homeostatically regulated by glycogenolysis by epinephrine and glucagon and glycogenosis by insulin. As I stated in Chaps. 10 and 12, glycogenolysis in liver and active glycolysis are metabolic hallmarks in cancer. However, an early preneoplastic event common to both chronic liver disease patients with a high risk for hepatocellular carcinoma and N-nitrosomorpholine-treated chemical hepatocarcinogenesis model in rats is glycogenotic activity that mimics the insulin effect [40]. This also can be recognized as a homeostatic response to a driving force for glycogenolytic activity that still is latent.

A similar phenomenon in angiogenesis is observed. Semaphorin3A (Sema3A) is one of the endogenous angiogenesis inhibitors by signaling through cellular cytoskeleton (see Chap. 16). In biopsy samples of human uterine cervical cancer patients, Sema3A was highly expressed in the epithelial cells and some endothelial cells in high-grade dysplasia called CIN-3, which was totally absent in cervical squamous cell carcinomas (SCC) [41]. This was supported by the HPV/E2 mouse model in which cervical tumor progression could be time-dependently observed from low-grade (CIN-1/2), CIN-3 lesions, and SCC. Sema3A was highly expressed

in endothelial cells in CIN-3 lesions. It is likely that the up-regulation of Sema3A is a homeostatic response against the angiogenic switch by the tumor before full tumor angiogenesis.

15.6.2 LPS Mimicry in Premetastatic Lungs

15.6.2.1 Roles of S100A8 (see Figs. 15.1–15.3)

The idea of LPS mimicry is based on the demonstration (see below) by us and other group that MD-2, the co-receptor of TLR4 (see Fig. 5.3 in Chap. 5), binds not only LPS but also S100A8 and SAA3.

In biochemical levels, we used full-length S100A8 and SAA3 proteins expressed in and purified from mammalian cells, and synthetic peptides of various lengths theoretically to avoid contamination of LPS. Surface plasmon resonance analyses revealed that Kd is 10 nM for mammalian S100A8 and 0.356 nM for mammalian SAA3 when tested with baculovirus-purified TLR4/MD-2 proteins [42]. The apparent Kd between TLR4/MD-2 and lipid A was 3 nM (see Chap. 5). The synthetic peptide of 2–89 amino acids of S100A8 binds MD-2 purified from baculovirus with Kd 0.73 μM and stimulated cell migration in vitro in a manner dependent on TLR4, MD-2, and MyD88. The binding domain is localized in the C-terminal 30 amino acids S100A8 [60–89], which is supported by the results of docking simulation [43]. Overlapping peptide scanning of 15 amino acids of SAA3 revealed that amino acids 43–57 bind the MD-2 with Kd 30 μM and stimulated cell migration dependently on TLR4, MD-2, and MyD88. Injection of the bioactive 15-mer to achieve a serum concentration around the Kd value in tumor-non-bearing mice could mobilize BMDC to the lungs in an MD-2-dependent manner [44].

When human peripheral mononuclear cells were stimulated by either 1 μg/ml of *E. coli*-derived LPS or purified S100A8 with endotoxin <0.01 pg/ml for 24 h and the culture supernatants were subjected to cytokine array, both induced for example CCL2 but IP-10 and CXCL12 were induced only by LPS. Cytokines specifically induced by S100A8 were not found [45].

The up-regulation of S100A8 and S100A9 in premetastatic lungs is dependent on VEGF and TNFα, both of which are produced by the primary tumor [46]. The lung metastasis is blocked by anti-S100A8 antibody or TLR40-KO. Let us consider pneumonia. LPS in the alveolar space promotes permeability in epithelial barrier. Anti-S100A8 antibody can suppress transepithelial migration of leukocytes from the interstitial to alveolar space. Given the bacteriocidal roles of leukocytes in the alveolar space, it is reasonable for bacteria to promote epithelial permeability for invasion and for leukocytes to counter-migrate. Because anti-S100A8 antibody can block transendothelial migration of leukocytes from circulation to interstitial space, S100A8 is likely to contribute to extravasation of leukocytes in physiological and of tumor cells in pathological condition.

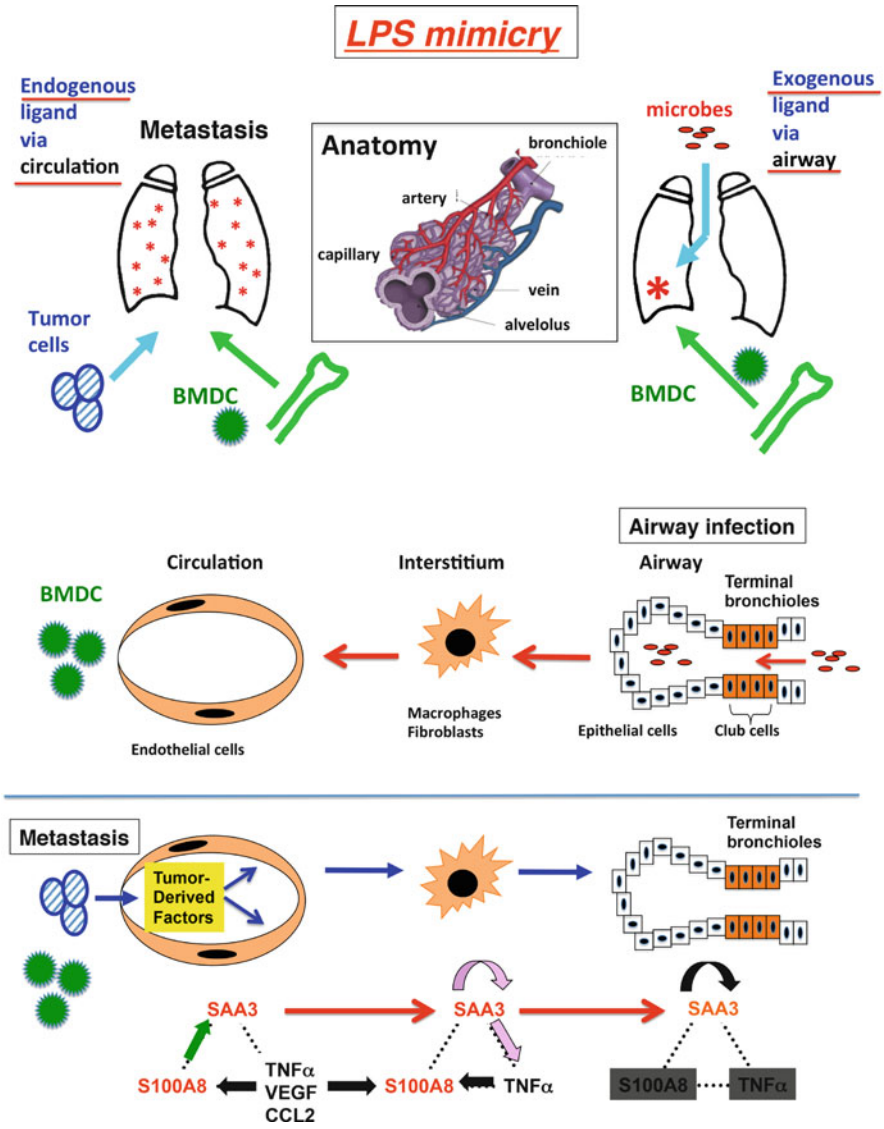

Fig. 15.2 LPS mimicry. Lungs have interphase between circulation and airway with paracrine signaling. Exogenously borne microbes through the airway induce mobilization of bone marrow-derived myeloid cells (*BMDC*) to the lungs. The triggering mechanism may involve microbial LPS that activates TLR4 in club cells in terminal bronchioles. The paracrine signaling goes in the direction to the circulation side. Expression of endogenous ligands, such as S100A8 and SAA3, in endothelial cells in sterile premetastatic lungs is induced by primary tumor-derived growth factors, such as CCL2, from the circulation side and the paracrine signaling goes in an opposite direction from the circulation to airway side to result in amplification of SAA3 in club cells. Bone marrow may misrecognize those endogenous ligands as LPS derived from lung infection and mobilize the myeloid cells there to battle against the phantom microbes

Leukocyte extravasation requires their initial attachment with endothelial cells. Bone marrow leukocytes are known to up-regulate Mac-1 (CD11b-CD18) expression in response to not only LPS but also other inflammatory factors including TNFα, LTB4, and C5a. In neutrophils, in which roughly 40% of cytosolic protein is S100A8 and A9, native S100A8-S100A9 heterodimers purified from neutrophils failed to enhance adhesion to fibrinogen whose receptor is Mac-1 at concentrations up to 2 μM, whereas *E. coli*-expressed S100A9 could do so by changing CD18 (=β2 integrin) into an active form that can be recognized by monoclonal antibody mAb24 [47]. If the recombinant S100A9 protein was contaminated by LPS, it should be the LPS activity via TLR4. If not, the activity should have been mediated by a receptor that binds S100A9 but not S100A8; the most likely one is CD147 (see below) whose activation results in expression of TNFα that may work in a paracrine fashion.

S100A8 and S100A9 were claimed to be in vivo substrate of MMP9 whose knockout reduced lung metastasis [48].

The Peter Angel group nicely engineered hepatocyte-specific conditional double transgenic mice of S100A8 and S100A9, which displayed no disease phenotypes including inflammatory lesions [49]. Both proteins were detected weakly in the liver but not increased in the serum from the baseline. Interestingly, they showed roughly twofold up-regulation of serum concentration of CXCL1 with systemic enrichment of $Gr1^+$ $S100A8^+$ monocytic cells in circulation and passively in liver. Given that S100A8 was up-regulated in the serum of tumor-bearing mice in our experiments, S100A8 induction of CXCL1 is sufficient for leukocyte mobilization from the bone marrow. I am eager to see if portal injection of $TLR4^-$ or RAGE-expressing cells can augment liver metastasis. For CXCL1, also refer to Chaps. 12 and 16.

Plasminogen activator inhibitor-1 (PAI-1) (see Chaps. 3 and 12), which is induced by LPS or ATF3 activation, plays a defensive role in pneumonia by facilitating transepithelial migration of leukocytes into the air space. Both S100A8 and SAA3 can potentially activate ATF3 (see below). Therefore, the defensive mechanism against bacteria by mobilizing leukocytes is <hijacked> by tumor cells. Just like leukocytes moving toward LPS, tumor cells move toward those endogenous TLR4 ligands in the lungs resulting in metastatic dissemination. PAI-1 inhibits plasminogen activator responsible for generating plasmin, which can activate MMP9 required for metastatic microenvironment. This seems paradoxical. However, S100A8 and SAA3 cause vascular permeability and fibrin-fibrinogen deposition, which as a next step activates fibrinolytic events.

15.6.2.2 S100A8 and the Eph-Ephrin System

S100A8 induces ephrin-A1 expression [50]. The original finding was that LPS induces TNFα, which then promotes expression of ephrin-A1 in HUVEC. The prototype of the Eph (The cDNA was originally isolated from a nude mouse transplantable tumor named erythropoietin-producing hepatoma) family of receptor

tyrosine kinases, now called EphA1, was discovered by me in 1987, and currently the family is grouped into EphA with ten members and EphB with six members. Their ligands are either GPI-anchored ephrin-A1 through A6 or transmembrane ephrin-B1 to B3 proteins, respectively. The system forms a counter-receptor system giving both forward (ephrin to Eph) and reverse (Eph to ephrin) signaling. The family members play important roles in many biological settings, including EphB4-ephrin-B2 in arteriovenous differentiation, ephrin-B2 in VEGFR2 activity, and EphA3/A5-ephrin-A2/A5 in neuronal pathfinding.

Systemic administration of LPS mimics bacterial assaults from the most exposed organs, i.e., lungs sensing air-borne LPS and liver responsible for perception of gut-derived LPS via portal vein. The misrecognition by those organs was reflected in the time-dependent up- and down-regulation of both EphA1/A2 and ephrin-A1 expressions, which is presumably involved in vascular permeability to allow leukocyte extravasation there [51]. A small elevation of LPS from whatever tissues attacked by bacteria is homeostatically controlled by this way.

We have shown that the EphA1and EphA2 can bind the membrane-bound ephrin-A1 in lung endothelial cells serving as adhesion molecules in a manner independent of its tyrosine kinase activity [52]. However, a soluble form of ephrin-A1, which is released from the primary tumor by ADAM12-mediated shedding, reaches in an endocrine fashion and disrupts the pulmonary vascular barrier disorganizing VE-cadherin. We also have shown that the ephrin-A1-Fc recombinant soluble protein causes contraction of endothelial cells in a tyrosine kinase-dependent manner through the SAM domain binding to integrin-linked kinase and the subsequent RhoA-ROCK pathway [53]. In both EphA1-KO and EphA2-KO mice, vascular permeability in the lungs was actually increased. The information indicates the disruption of molecules that usually participate in lung homeostasis as adhesion machinery causes inflammation in the lungs, i.e., vascular permeability and cell migration. The critical mechanism is likely switching between on and off state of the EphA1 tyrosine kinase activity.

Therefore, the mechanisms of premetastasis cannot be explained without putting into consideration of molecules directly involved in lung homeostasis. The classical danger, such as invading bacteria or tumor cells and necrotic cells, are absent in the premetastatic lungs, but both vascular permeability and cell migration actively take place as in the case of physiological conditions. However, their levels are higher than those in physiological circumstances (see below). After arrival of tumor cells, which is the true danger, danger hypothesis-based events continue as found in the primary tumor.

15.6.2.3 A Single Match Can Start Fire

What is the mechanism by which to explain the sustained expression of S100A8 and SAA3 in the lungs while their serum levels decrease 10–14 days after implantation of tumor cells? Detailed analysis of stimulation and expression pattern of S100A8, SAA3, and TNFα revealed that the triggering mechanism is primary tumor-secreted

CCL2 that activates CCR2 in the hyperpermeable regions in the lungs to induce S100A8 expression in the endothelial cells. S100A8 from endothelial cells is secreted into the interstitium where macrophages are located and stimulated to secrete SAA3. The interstitial SAA3 then stimulates TLR4 expressed in club cells in the terminal bronchiole regions, a preferential site of lung metastasis. Club cells then express SAA3, which stimulates their own TLR4 resulting in autoamplification of SAA3 [54] (Fig. 15.2). At this stage, the paracrine cascade starting from CCL2 may be dispensable for the establishment of premetastatic milieu even if the primary tumor is removed. It is assumed that TLR4 inhibition may be one of the reasonable ways to put an end to the SAA3 autoamplification.

An initial LPS exposure is known to induce tolerance against subsequent LPS challenge. The mechanisms involve TLR4-induced activation of aryl hydrocarbon receptor (AhR) whose ligands include dioxin of environmental origin and endogenous kynurenine, a product of tryptophan catabolism by indoleamine 2,3-dioxygenase 1 (IDO1) that also is induced by TLR4 activation, as manifested by deceased serum levels of TNFα and IL-6 [55]. AhR-KO mice were more sensitive to endotoxemia by impaired mitigation of the TLR4-NFκB signaling by AhR. AhR is expressed in club cells that metabolize xenobiotics and can autoamplify SAA3. By utilizing AhR-expressing primary hepatocytes derived from AhR-KO mice, it was shown that a potent AhR agonist TCDD (2,3,7,8-tetrachlorodibenzo-p-dioxin) repressed SAA3 expression induced by IL-1β and IL-6 [56]. The authors showed that similar effects were observed with different AhR agonists, such as benzopyrene and naphthoflavone, and that the mechanisms involved inhibited recruitment of p65RelA and C/EBPβ to the SAA3 promoter. However, ongoing studies in our laboratory have shown that neither S100A8 nor SAA3 lack this feedback (Tsukahara and Maru, unpublished results).

Readers should remember that CCL2 is also involved homeostatic inflammation in alveolar recruitment of monocytes (see Chap. 14). We have shown that both S100A8 and CCL2 can induce vascular permeability in the lungs. I will review interesting experiments by Jeffrey Pollard group [57]. They defined inflammatory $Ly6C^+$(therefore $Gr1^+$) (see Chap. 12.6.3.2) and resident $Ly6C^-(Gr1^-)$ monocytes sharing $CD45^+CD11b^+CD115^+$ phenotypes (CD115 is $CSF1^-R$ and almost all $CD115^+$ cells are $Ly6G^-$), which were sorted from CSF1-R-GFP transgenic mice to track down after adoptive transfer into MMTV-PyMT mice. While $Gr1^-$ monocytes were recruited in the primary tumor, $Gr1^-$ monocytes were mobilized to the late-stage lung metastatic lesions and forced pulmonary metastatic nodules by intravenous injection of a PyMT-induced mouse mammary tumor cell line (Met-1), and intriguingly lungs 7 h after intravenous injection of Met-1 cells before extravasation in the lungs, but not 7-week-old PyMT mice with yet premalignant mammary tumors presumably without expression of CCL2 even if they make an entry into circulation. High levels of CCR2 expression were observed in the recruited $Gr1^-$ monocytes. Notably, CCL2 expression levels in tumor cells were homogenous in the metastatic lung nodules but heterogenous in the primary tumor. Therefore, CCL2 expression appears to confer a metastatic trait on the tumor cells. Given that even CTC expressing CCL2 alone without primary tumor induced $Gr1^+$

monocytes in the lung, augmented levels of CCL2 in circulation may be misrecognized by $Gr1^+$ monocytes in the bone marrow as a danger producing CCL2 in the lungs. The recruited monocytes are destined to prepare premetastatic soil by producing VEGF in contact with CCL2-secreting tumor cells and VEGF works in concert with CCL2 to facilitate tumor cell extravasation into the lungs. They showed that myeloid cell-specific conditional knockout of VEGF by the tamoxifen-inducible system linked to the CSF1-R promoter abrogated the tumor cell seeding in the lungs. VEGF by itself was not required for the recruitment of $Gr1^-$ monocytes since VEGF-null monocytes were recruited at similar levels to the control.

15.7 TLR4-Deficient Phenotypes

TLR4 is a double-edged sword but seemingly defensive.

The TLR4 polymorphism D299G in the extracellular domain showed reduced LPS response with a greater risk of sepsis and decreased ability for binding HMGB1, an endogenous TLR4 ligand (see Part II). The frequency of metastasis by 5 years after breast cancer surgery was 40% in D299G patients compared with 26.5% in those without polymorphism, suggesting the polymorphism is loss of defensive function [58]. Autosomal recessive mutations in MyD88 within the IRAK4-interacting domain, such as L93P result in failed interaction with IRAK4 leading to severe infection with pyrogenic bacteria during the early infancy [59]. Compared with reactions in the initial exposures to exogenous bacteria in neonates, those in early adolescence get less and less severe. Conversely, a gain of function mutation L265P in MyD88, which results in constitutive MyD88 signaling with production of cytokines, such as IL-6, can facilitate diffuse large B-cell lymphoma progression [60]. Thus, the TLR4-MyD88 pathway appears to be defensive against bacteria and tumor progression, but too much defensive reaction favors tumor progression.

LPS reduces the expression of CCL21 through the TLR4-SOCS3 pathway in high endothelial venules in lymph nodes, which results in less mobilization of CCR7-expressing lymphocytes as attackers to the lymph nodes [61]. In this case, TLR4 weakens the defense via CCL21. When tumor cells express CCR7, CCL21 promotes their mobilization through afferent lymphatic ducts that are dilated by VEGF-C. Here, CCL21 promotes the attack. In both cases, it is favorable for attack by tumor cells.

This apparent discrepancy can be easily understood by thinking of homeostatic mimicry and the hijacking idea. LPS mobilizes defensive BMDC. S100A8 also mobilizes defensive BMDC [62]. Mobilized BMDC participates in more S100A8 production but find no enemy or attackers to battle against in the premetastatic lungs. Overexpressed S100A8 mobilizes aggressive tumor cells expressing TLR4 in postmetastatic lungs. An siRNA-mediated knockdown of TLR4 in tumor cells

abrogated their lung metastasis [54]. At this stage, defenders are substituted with attackers.

TLR4 activation inhibited growth of breast cancer cells with wild-type p53 by increasing growth-suppressing IFNγ secretion but promotes growth of those with p53 mutations by expression progrowth cytokines, including IL-6 and CXCL1 [63].

As I just stated, both plasma S100A8 and SAA3 elevate in tumor-bearing mice 10 and 8 days, respectively, after subcutaneous implantation of tumor cells with recruitment $CD11b^+$ myeloid cells in the premetastatic lungs. There are some differences between intravenously injected LPS and the endogenous TLR4 ligands produced in tumor burden. Reciprocal BMTs between wild-type and $TLR4^-$KO mice can theoretically generate (1) BM TLR4-KO with most of the pulmonary population of cells, such as epithelial and endothelial cells are of wild-type, and (2) lung $TLR4^-$KO with recruitment of a small population of wild-type cells from the bone marrow. When systemic LPS was administered at 0.5 mg/kg, neutrophil recruitment in the lungs was observed within 4 h as monitored by myeloperoxidase activity and chloroacetate esterase staining in the lungs, which was abrogated in $TLR4^-$KO and lung $TLR4^-$KO, but not BM $TLR4^-$KO, E- and P-selectin double KO and CD18-KO [64]. LPS-activated TLR4 was reflected in the P-selectin expression in the lungs in totally wild-type and BM $TLR4^-$KO mice but not $TLR4^-$KO and lung $TLR4^-$KO mice. Collectively, LPS stimulates TLR4 expression in the lung resident cells to induce neutrophil recruitment.

When similar experiments were performed by tumor challenge, which increases plasma levels of both S100A8 and SAA3, pulmonary recruitment of $Mac1^+$ myeloid cells was impaired in $TLR4^-$KO and BM $TLR4^-$KO mice but not lung $TLR4^-$KO mice, indicating that blood cell TLR4 is important, but the experiments failed to reduce the significance of lung TLR4. Because club cells, which express TLR4, are derived from BM, a mixture of $TLR4^+$ and $TLR4^-$ club cells was present in lung $TLR4^-$KO mice.

15.8 S100 Family

More than 20 members are known in the S100 family proteins [65]. They are homologous to each other by 25–65% in amino acid levels. Information of the members with determined crystal structure revealed that they have an EF-hand motif and form antiparallel homo- or hetero-dimers. They can further associate to form high-order multimers. High-resolution NMR spectroscopy revealed that binding of Ca2+ opens up the hydrophobic pocket allowing their interaction with the C-type immunoglobulin domain of RAGE, i.e., Ca2+ molecularly switches the binding. This Ca2+ sensor is engaged in a variety of biological events by functioning in intracellular and/or extracellular space.

S100A8 can preferably form a hetero-dimer with S100A9. In peripheral blood cells from S100A9-KO mice, S100A8 proteins were under detection, although S100A8 mRNAs were present, suggesting that S100A9 proteins are responsible

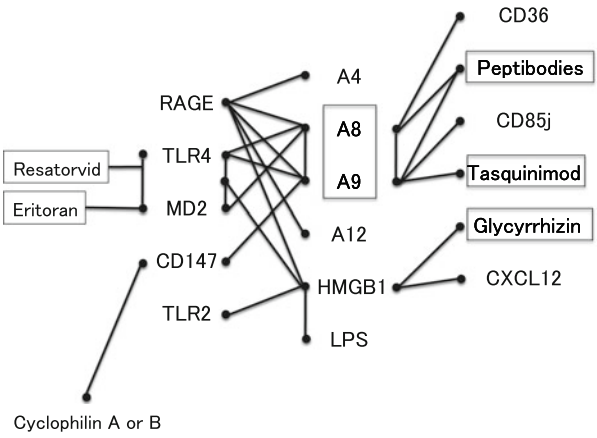

Fig. 15.3 Multiligand/multireceptor system

for stabilization of S100A8 proteins in mice [66]. An opposite situation was reported in humans. Human S100A9 proteins were unstable in the absence of S100A8 proteins [67]. Both S100A8 and S100A9 proteins were initially identified in the synovial fluid of rheumatoid arthritis patients [68].

Corpora amylacea in prostate glands of prostate cancer patients mainly consists of amyloid (see Chap. 6) of S100A8 and S100A9 [69]. S100A8/S100A9 proteins purified from granulocytes showed a propensity to aggregate in vitro forming fibrillar structures in 8 weeks in a manner dependent on Zn2+ and Ca2+ as judged by atomic force microscopy and transmission electron microscopy [70]. Liquid chromatography-electrospray ionization mass spectrometry of corpora amylacea revealed the presence of hemoglobin subunits and myeloperoxidase of host origin as well as bacterial DNA sequences, strongly indicating the involvement of bacterial infection-induced inflammation in the formation of this crystal.

S100A8 expression is up-regulated not only in pre-metastatic lungs but also in synovial fluid in rheumatoid arthritis patients, serum from SLE and intestinal epithelial cells of Crohn's inflammatory bowel disease and most importantly in tumors [71, 72].

In contrast to most secretory proteins exported by the ER-Golgi pathway, unconventional, i.e., still unknown mechanisms underline the release of IL-1β, IL-18, IL-33, proIL-1α, FGF, and S100A8, all of which lack the leader sequence [73]. It is known that IL-1β secretion depends on NARLP3 inflammasome and caspase-1 activation [74].

In addition to soluble factors, such as TNFα and LPS, HIF-1 induces expression of both S100A8 and S100A9 by binding to their hypoxia response element (HRE) in the promoters in benign prostate epithelial hyperplasia BPH-1 cells and prostate cancer PC-1 and DU-145 cells [75]. Analysis of 145 patients who were subjected to radical prostatectomy revealed similar expression patterns of S100A8 and HIF-1α in immunostaining and a negative correlation between the expression levels of S100A9 and the time required for recurrence.

Although dexamethasone alone failed to induce S100A8 expression in 20 h but enhanced LPS-stimulated expression in thioglycolate-elicited murine macrophages, it directly induced S100A8 expression in human blood monocytes. Synovial knee joint biopsy of RA patients revealed that S100A8-positive cell numbers increased 24 h after intravenous administration of methylprednisolone [76]. Up-regulation after steroid may imply that S100A8 is at least seemingly anti-inflammatory. However, the story is not so simple. For example, increased expression of S100A8 in acute lymphoblastic leukemia with MLL gene translocation confers glucocorticoid resistance on the patients. In this case, abundant intracellular S100A8 is assumed to interfere with glucocorticoid-elicited Ca2+ fluxes from the ER to mitochondria [77].

Two receptors are known for S100A8: TLR4 and RAGE [78, 79] (Fig. 15.3). More precisely, we showed that S100A8 binds the MD-2 coreceptor of the TLR4-MD-2 complex. Only N-glycosylated RAGE, which constitutes only 5% of total RAGE, can bind S100A8 [80]. From the RAGE side, it can bind the authentic ligand AGE, S100A6, and S100A12 [81, 82]. One of the unique features of S100 proteins is that they lack signal peptides usually essential for secretory proteins, but they are actually secreted actively and passively into the extracellular space by an as yet unknown mechanism.

Members that participate in tumor biology include S100A2, S100A4, S100A6, S100A7, S100A8, S100A9, and S100B [83]. Clinical correlation between the expression and invasive levels has been reported in S100A4 (also called metastasin) in particular. This is supported by two logical experiments, i.e., metastasis in MMTV-neu mice was enhanced when crossed with S100A4 transgenic mice, while that in MMTV-PyMT with S100A4-KO was suppressed, indicating that S100A4 is necessary and sufficient for the tumor metastasis although the mechanism is still unclear [84]. Both stromal cells and tumor cells are influenced in terms of expression levels of S100A4 in those tumor models.

Similar to S100A8, it is abundant in the synovial fluid of rheumatoid arthritis patients and in the psoriatic skin. Intraperitoneal administration of anti-S100A4 antibody in the human psoriasis xenograft in SCID mice was effective by reducing the epidermal thickness and Ki-67+ proliferating cells [85]. While expression of S100A4 in tumor cells induces their metastatic potentials, various types of cells, including T cells, DC, macrophages, fibroblasts, and myofibroblasts, are S100A4-positive in psoriatic skin. Secreted forms of S100A4 are thought to bind RAGE.

15.9 Issue of Multiligand/Multireceptor System

S100A8 and S100A9 can form homo-dimers and hetero-dimers, but their partial synthetic peptides do not necessarily do so (Fig. 15.3). I mean either monomer or homo-dimer by S100A8 and heterodimer by S100A8/S100A9. In 1999, Marion

A. Hofmann initially showed evidence of a linkage of S100 family with inflammation by S100A12 binding to RAGE whose authentic ligand is AGE (see Chap. 6) pathologically essential in diabetes mellitus [82]. Mice lack the S100A12 gene of which S100A8 may function in place.

In a skin carcinogenesis model induced by chemicals DMBA/TPA, S100A8, S100A9, MIP-1α, MIP-1β, and MIP-2 were up-regulated [86]. Those are target genes of NFκB that is activated by RAGE or TNFα. Knockout mice of either TNFα or RAGE were resistant to this chemical carcinogenesis, suggesting sustained NFκB activation by a positive feed-forward loop of S100A8/S100A9 to RAGE to NFκB to S100A8/S100A9. Reciprocal BMT experiments with wild-type and RAGE-KO mice revealed that RAGE in bone marrow cells is responsible for carcinogenesis and dermal infiltration of neutrophils and macrophages. Now RAGE has at least five ligands, i.e., AGE, S100A6, S100A12 (only human), S100A8/S100A9, and HMGB1. Conversely, S100A9 has at least three receptors: RAGE, TLR4, and EMMPRIN.

Tomas Leanderson group has shown that human S100A9 and dimeric S100A8-S100A9 bound human RAGE with KD of 38 nM and 9.4 nM, respectively [87]. It is of note that S100A12 bound RAGE with KD at 90 nM. They also bound the human TLR4-MD-2 complex with KD of 2.1 nM and 3.8 nM, respectively. Because the binding was not inhibited by simultaneous application of MD-2 proteins, it is likely that S100A9 binds the TLR4 side.

Affinity isolation as spectrometry in search of binding proteins for S100A9 identified EMMPRIN also called CD147 [88]. S100A9 stimulation induced expression of CXCL1, TNFα, ephrin-A1, and MMP1 in the EMMPRIN signaling presumably via TRAF2. RAGE, another receptor for S100A9, failed to form a heterodimer with EMMPRIN. Intravenously injected EMMPRIN-expressing melanoma cells metastasized to the skin of S100A9 but not S100A8 transgenic mice with the epidermis-specific involucrin promoter.

Furthermore, pull-down experiments of human monocyte-derived dendritic cells after HIV-1 infection with Fc-fused CD85j, which belongs to the human leukocyte immunoglobulin-like receptor family, revealed binding of S100A9 [89]. They reported that stimulation of purified NK cells by recombinant tetrameric but not monomeric S100A9 proteins expressed and purified from *E. coli* in endotoxin-free conditions as they claimed increased production of TNFα and enhanced their anti-HIV-1 activity.

15.10 Endogenous Modulators

If homeostatic, LPS should have a feedback loop. See Fig. 5.3 in Chap. 5 for the fundamental TLR4 signaling cascade.

15.10.1 A20

Negative regulation by A20 was stated in Chap. 8.

15.10.2 ATF3

In addition, upon TLR4 activation, NFκB-mediated ATF3 transcription takes place [90]. ATF3 directly associates with HDAC1 to inhibit TLR4-driven gene expression [90]. Although LPS stimulation induced expression of neutrophil chemoattractant CXCL1 in ATF3-KO mice, neutrophil recruitment in the ATF3-KO lungs was not observed [91]. Gene expression profile analysis revealed that TIAM2 was down-regulated in ATF3-KO, which was responsible for the migration defect.

In the OVA-induced model of bronchial asthma, ATF3 is up-regulated in the lungs. ATF3-KO increased the hyperresponsiveness, pulmonary eosinophilia, and Th2 cytokine production [92]. When you remember this model combined with lung metastasis by B16F10 melanoma cells (see above), you would expect aggravation of metastasis in the lungs. However, myeloid specific ATF3-KO or general ATF3-KO both reduced lung metastasis in the background of syngeneic orthotopic MMTV-PyMT mammary cancer model [93]. Interestingly, there was no difference in the primary tumor growth. Transcription factor ATF3 is activated in a variety of cells essentially by stress, such as hypoxia, IL-6, and TNFα. ATF3-activated macrophages, for example, switch the balance to M2 and directly activate MMP9 expression. This may be one reason to explain the metastasis-suppressing activity in the ATF3-KO mice.

15.10.3 CD11b

Activated TLR4 also induces PI3K- and RapL-mediated activation of CD11b, i.e., changing its conformation from an inactive to active state. As you remember that CD11b is an integrin αMβ2, this is an inside-out signal. This elicits a sequential activation of Src and Syk associated with ITAM [94]. Then Syk phosphorylates MyD88 and TRIF, to which an E3 ligase Cbl-b binds and ubiquitinates for proteasomal degradation. This eventually weakens the LPS-induced signaling by CD11b-mediated negative feedback.

15.10.4 Calcineurin

Calcineurin inhibitor, such as FK506, or an siRNA-mediated knockdown of calcineurin in RAW cells augmented the TLR4-NFκB cascade-mediated expression of TNFα [95]. Conversely, a constitutively active calcineurin by deleting the autoinhibitory and calmodulin-binding regions reduced LPS-stimulated activation of NFκB. Given that TNFα production by FK506 was reduced in macrophages deficient in MyD88, TRIF, TLR4, and TLR2 and that calcineurin co-immunoprecipitates with them, the mechanisms may involve interaction, direct or indirect, between calcineurin and those molecules.

15.10.5 Akt

LPS activates Akt. While TRAF6 located downstream of TLR4 signaling can serve as a direct E3 ubiquitin ligase for Akt important for its membrane translocation and activation in growth factor-activated tumor cells, Akt controls regulatory microRNAs [96]. For example, Akt up-regulates miRNA let-7e that is capable of repressing TLR4 expression within a few hours, which is restored to the baseline in 48 h. Akt1-KO macrophages displayed exaggerated responses to LPS.

15.11 SAA3 Exists in Humans

The deduced amino acid sequence portion between mouse and human SAA3 are highly homologous to each other, and a single nucleotide insertion in the human SAA3 exon2 results in a frameshift to generate a shorter SAA3 with a unique C-terminal SAA3 sequence of 12 amino acids. Interestingly, this type of evolutionary genetic alteration occurs in primates, including chimpanzees (Fig. 15.4). Because no expression of human SAA3 has been reported so far, it has been assumed to a pseudogene. Although we could not find human SAA3 transcripts in the database of the expressed pseudogenes in tumor cells [97], elaborate qPCP analysis of human lung cancer samples in our laboratory revealed that there exists a chimeric SAA2-SAA3 fusion mRNAs [98]. The human SAA2 exon3 is connected to the human SAA3 exon2 with roughly 200 kb between the 2 exons to yield the SAA2-SAA3 fusion protein that could be recognized by a monoclonal antibody against the unique sequence of human SAA3. The corresponding gene product activates Erk by binding and stimulating LOX-1, an endothelial cell-specific scavenger for oxidized LDL. The binding affinity was 206 nM as judged by ELISA between C-terminal synthetic 26-mer human SAA3 peptide and soluble LOX-1. Given that neither the SAA2-SAA3 purified from mammalian cells nor synthetic

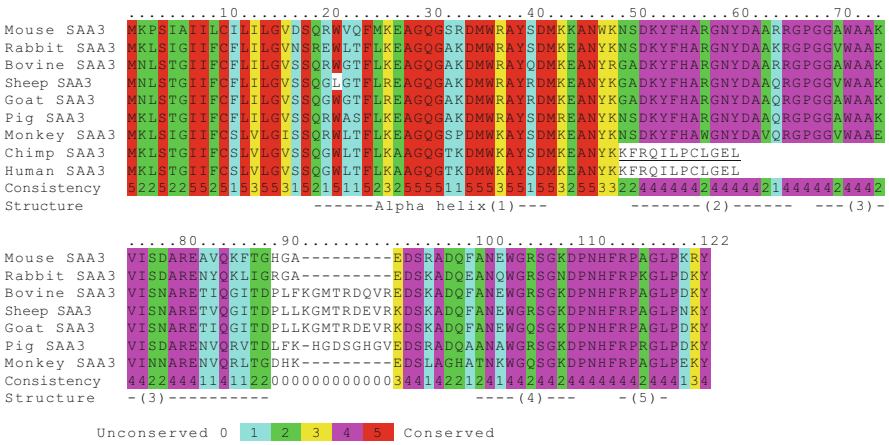

Fig. 15.4 SAA3 protein alignments in various species
SAA3 protein sequences are conserved in 56% except for those of chimpanzee (Chimp) and human. The amino acids are deduced from the corresponding genomic sequences that contain one base insertion generating a frame shift and truncated protein if expressed. The human SAA3 gene is believed to be a pseudogene

peptide of human SAA3 bound the TLR4-MD-2 complex, human SAA3 signaling is diverged from that of mouse.

15.12 Neonatal Switch from Bacteria to Endogenous Mediators

Exogenous LPS of initial encounter induced expression of CCR2, which in turn bound endogenous CCL2 in germfree mice, suggesting that innate stimulation by exogenous microbes induce receptors for endogenous mediators (Hiratsuka and Maru, unpublished data).

We have observed up-regulation of individually $CCL2^+$ and $CCR2^+$ cells in the lungs of LPS-treated but not PBS-treated germ-free neonatal mice. However, neonatal mice housed in the standard SPF conditions, in which they were exposed to LPS-containing bacteria, increased numbers of $CCL2^+$ and $CCR2^+$ cells were recognized even PBS-treated mice. In the SPF neonates LPS administration followed by LLC injection induced the tumor cell recruitment in the lungs, which was totally abrogated in CCR2-KO mice (Hiratsuka and Maru, unpublished data). Thus, neonatal exposure to exogenous LPS activates the CCL2-CCR2 system, which leads to the endogenous TLR4 cascade of the S100A8-SAA3 paracrine system.

A similar situation is known in SAA3 expression in adipose tissue through gut [99, 100]. Levels of SAA3 mRNA in epididymal adipose tissue and colon of germ-free Swiss-Webster mice were approximately ten- and sevenfold, respectively, higher than those raised conventionally. MyD88-KO reduced the SAA3 mRNA levels by sixfold compared with the wild type. LPS simulates TLR4 in the colon epithelial cells as well as macrophages to induce SAA3 expression. Serum levels of SAA3 in conventionally raised mice were higher than those in germ-free mice and LPS administration induced SAA3 expression in adipose tissue. Given that both authentic ligand LPS and endogenous one SAA3 bind TLR4 in adipose tissue macrophages to secrete SAA3 by a feed-forward mechanism. Thus LPS-triggered and autoamplified SAA3 production stimulates myeloid cell mobilization from bone marrow resulting in accumulation of macrophages in both tissues. The inflammatory response in both colon and adipose tissue is stabilized at homeostatic levels. We should pay attention to the mechanism by which LPS-induced inflammation in colon can spread to other tissue(s) if LPS can induce expression of endogenous TLR4 ligands, because they can function as LPS in bacteria-free tissues.

15.13 MDSC and Premetastasis

What are the roles in premetastatic lungs of MDSC that I stated in the Chap. 12? In our initial report of premetastatic lung establishment by S100A8, we monitored Mac-1^+ cells. This population of cells includes $CD11b^+$ $Gr1^+$ cells, i.e., MDSC. In breast cancer ectopic xenograft model with 4T1 cells labeled by GFP, which causes spontaneous metastasis to the lungs, flow cytometric analysis and qPCR analysis of GFP of the lungs showed that mice did not have tumor cells in the lungs until 14 days after tumor implantation. Coculture of sorted MDSC with normal lung cells revealed that the number of IFNγ-producing macrophages was significantly decreased [101]. Histological analysis of the premetastatic lungs showed that costaining of $CD11b^+Gr1^+$ and $MMP9^+$ cells. In addition, HUVEC cocultured with MDSC producing MMP9 disrupted VE-cadherin of HUVEC.

It is likely that MDSC cultivates the soil by reducing antitumor effect and by promoting pulmonary vascular permeability.

MDSC accumulate not only in the premetastatic lungs but also in other parts of the body, such as the spleen, by more than fivefold in 3 weeks after tumor cell transplantation. Analysis of the splenic population of MDSC revealed several interesting features: (1) MDSC failed to accumulate in tumors transplanted in S100A9-KO mice but instead $CD8^+$ and $CD4^+$ T cells infiltrated the tumor and 9 of 12 mice rejected tumor; (2) S100A9 overexpression induced MDSC accumulation by blocking myeloid differentiation via the Nox2 complex-mediated production of ROS.

Is S100A8-SAA3 expression necessary and/or sufficient for premetastatic soil establishment? Both anti-S100A8 and anti-SAA3 antibodies individually blocked lung metastasis as we reported previously [42, 46]. SAA3-KO mice showed no prominent phenotypes in metastasis experiments in our hands (Tomita T and Maru Y, unpublished results). Because S100A8-KO mice were embryonic lethal, we are currently trying to establish conditional S100A8-KO mice to uncover the homeostatic role of S100A8.

We have discussed on inflammatory conditions, including LPS administration and acute pneumonia, which promote lung metastasis. Knockout mice of uteroglobin, which is an anti-inflammatory protein also called CCSP or CC10 (see Chaps. 14 and 15), a specific marker of lung club cells, displayed up-regulated expression of lung S100A8 and enhanced lung metastasis when injected with B16F10 melanoma cells through the tail vein in a tumor nonbearing condition [13].

In mice with keratin 5-directed expression of IκBα to the epidermis (K5- IκBα), inflammatory hyperplasia with $S100A8^+$ neutrophil that dominated over $F4/80^+$ macrophages took place followed by the development of well-differentiated squamous cell carcinomas at 4 months of age. Up-regulation of TNFα, S100A8, and SAA3 was found in the skin lesions, which were sensitive to UVB at 500 J/m^2 to induce apoptosis [102]. The dermatitis and skin tumor formation were abrogated when K5- IκBα mice were crossed with TNFR1-KO but not CCL2-KO mice [103, 104]. Murine mammary cancer Met1 cells were subcutaneously implanted in K5-IκBα mice, and the tumor was resected to promote lung metastasis. In premetastatic lungs, $CD11b^+Gr1^+$ cell numbers were elevated but reduced after the resection. However, the resection induced development of macroscopic metastatic nodules in the lungs but not in the skin where premetastatic factors that we proposed, such as S100A8 and TNFα, were constantly up-regulated (Tomita, Toftgard and Maru, unpublished data). Lung metastasis after resection can be explained by elimination of negative angiogenic switch on the tumor cells that reached the lungs before resection. However, the tumor cells could hardly reach the inflammatory skin, suggesting the presence of organotropic factors that control the lung metastasis.

15.14 Hijacking the RANKL-RANK System

Binding of receptor activator of nuclear factor kB (RANK) in osteoclast precursors and RANK ligand (RANKL) in osteoblasts induces osteoclast differentiation in the presence of M-CSF [105] (Fig. 15.5). The osteoclast precursors are derived from bone marrow hematopoietic stem cells and $c\text{-}Kit^+$ $M\text{-}CSFR^+$ CD11b low. This homeostasis in bone is hijacked by tumor cells to achieve bone metastasis by ectopically expressing both RANKL and RANK [106].

RANK stimulation elicits signaling through Akt and ERK, inducing cell migration but not cell proliferation or cell death. RANK is frequently expressed in breast

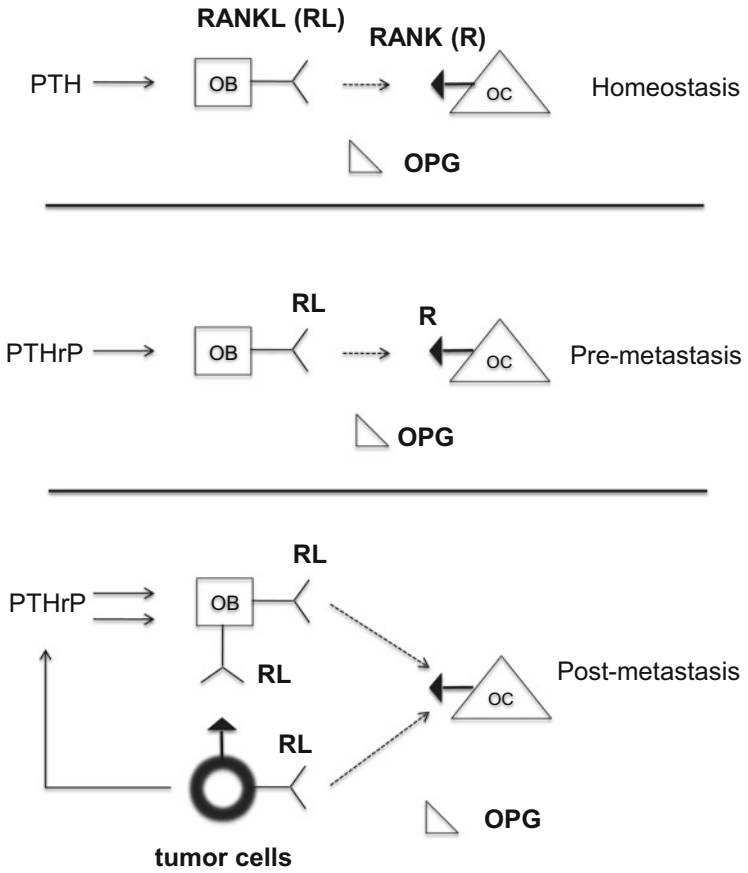

Fig. 15.5 RANK-RANKL in bone metastasis

and renal cell cancer [107]. RANK is also expressed in normal mammary gland epithelial cells. A report of 73 clear cell carcinoma of kidney showed that RANK, RANKL, and the soluble form of decoy receptor for RANKL called osteoprotegerin (OPG) were expressed in 82%, 66%, and 71%, respectively, as judged by immunostaining. Although roughly 30% of renal cell cancer patients develop bone metastasis, OPG-high patients were free of bone metastasis. Patients with strong expression of both RANK and RANKL had extramedullary metastasis to skin and liver.

RANK-expressing tumor cells migrate towards RANKL-expressing osteoblasts in bone. On arrival, RANKL in tumor cells and induced RANKL in osteoblasts by tumor cell-derived PTHrP stimulate RANK to induce active osteoclastogenesis and subsequent osteolytic bone metastasis. Given that RANKL is induced by LPS in

osteoblasts, endogenous TLR4 ligands, such as S100A8, derived from either myeloid cells or tumor cells might play a role in osteoclastogenesis [108].

Intracardiac injection of B16F10 melanoma cells that express high levels of RANK resulted in metastasis in bones, ovaries, adrenal glands, and brain. OPG not only inhibited RANKL-dependent cell migration of tumor cells in vitro but also suppressed bone metastasis in vivo. Intriguingly, however, metastasis to other organs was not affected. This information indicates that hijacking the RANK-RANKL system participates not only in the mobilization of tumor cells but also in organ specificity in metastasis.

In addition to tumor cells, LPS-activated TLR4-expressing neutrophils express RANKL. This also is the case in neutrophils from the synovial fluid of exacerbated rheumatoid arthritis patients in which endogenous TLR4 ligands S100A8 and S100A9 are abundant [109]. Therefore, RANKL not only in tumor cells but also in neutrophils participates in osteoclastic bone resorption.

COX-2 expression (see Chap. 1) is observed not only in a variety of tumor cells but also stromal cells. LPS induces PGE2 production in macrophages. In postmetastatic bone experiments with melanoma cells, we have shown by using coculture systems and gene knockout mice that B16 melanoma cell-osteoblasts contacts resulted in osteoblastic expression of RANKL in a membrane-bound (m) PGES-1 (see Chap. 1)-dependent manner, leading to osteoclast formation [110]. Bone metastasis was abrogated in genetic background of mPGES-1-KO or in the presence of an EP4 antagonist AE3-208 when melanoma cells were injected intravenously through the tail vein. Thus, in this case the RANK-RANKL system is hijacked by melanoma cell-stimulated activation of mPGES-PGE2-EP4 signaling in osteoblasts.

15.15 Connexin Hijacking

Another way to hijack homeostasis is found in one of the mechanisms of brain metastasis by breast cancer and melanoma. Connexin43 mediates homocellular communications in endothelial cells (see Chap. 3). Endothelial cell-specific knockout of connexin43 resulted in dramatic NO elevation and hypotension suggesting that vascular gap junctions contributes to vascular homeostasis [111]. Intraperitoneal injection of LPS into mice also induced bladder connexin43 expression in bladder smooth muscle cells, which was largely blocked by an iNOS inhibitor. This suggests complicated mechanisms of connexin43 expression in a variety of cells in which NO generation systems are involved [112].

An EMT regulator Twist up-regulates connexin43 expression in breast cancer cells, which mediates heterocellular communication between the cancer cells and brain endothelial cells [113]. The heterocellular connection appears to be functional as judged by the passage of calcein orange dye from the tumor cells to the brain endothelial cells, which might exchange other bioactive molecules. Importantly, using 4T-1 breast cancer cells that were labeled with PKH26 membrane dye, which

is retained when labeled cells are not dividing but lost after three cell divisions, the authors showed that the metastatic tumor cells that initiated heterocellular communication with brain endothelial cells may be dormant cells as exemplified by cancer stem cells.

15.16 Hormonalization of Autacoids

Autacoids function in a paracrine fashion in physiological conditions. However, when overexpressed in pathological conditions they appear in the blood stream and affect the distant target cells in an endocrine manner.

Autocrine secretion of VEGF in endothelial homeostasis, that of S100A8 in myeloid cells as exemplified in immune suppressive functions of MDSC and paracrine secretion of TNFα within a variety of tissues are known. Plasma levels of those factors increase in tumor patients in general, which allows their action in tissues distant from the sites of original overproduction, i.e., primary tumors.

For example, S100A8-A9 protein levels in plasma were elevated in gastric cancer patients [114]. Although the S100A8-A9 producing primary tumor is fixed in stomach, the plasma S100A8-A9 works in an endocrine manner to stimulate bone marrow-derived MDSC, which secretes S100A8-A9 forming an autocrine loop. MDSC circulate and migrate to a tissue including the primary tumor and distant ones apart from it, in which the original functions of S100A8-A9 are transmitted.

15.17 Premetastasis Precedes Danger (Damage)

In the danger theory, Matzinger proposed that the immune system is activated by damaged cells (Fig. 15.6) [115]. This led to the molecular identification of damage signals by so-called alarmins or danger-associated molecular patterns (DAMPs), including uric acids, HMGB1 (see Chap. 6), and S100A8 (Chap. 15). Although Matzinger described by mistake that the immune system fails to be activated by tumors, because they usually do not become necrotic to give DAMPs [116], current understanding is that tumors cause tissue damages and therefore premetastasis, which is devoid of tissue damages, precedes the arrival of tumor cells as a true danger.

15.18 Concluding Remarks

Hijacking of homeostatic roles played by endogenous mediators by tumor cells gives inflammatory conditions in premetastatic tissues.

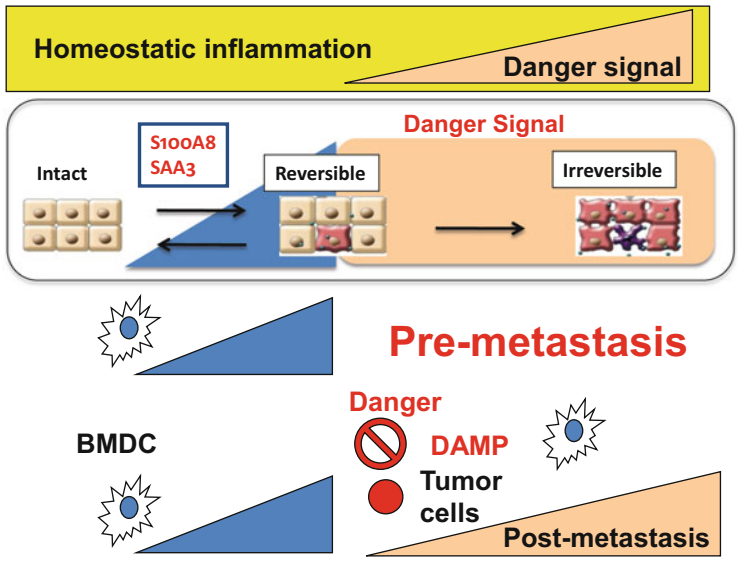

Fig. 15.6 Danger theory and premetastasis
Establishment of premetastatic milieu precedes damages caused by the arrival of metastasizing tumors as a true danger

References

1. Biswas S, Guix M, Rinehart C, et al. Inhibition of TGF-β with neutralizing antibodies prevents radiation-induced acceleration of metastatic cancer progression. J Clin Invest. 2007;117:1305–13.
2. Bald T, Quast T, Landsberg J, et al. Ultraviolet-radiation-induced inflammation promotes angiotropism and metastasis in melanoma. Nature. 2014;507:109–13.
3. Augustin G, Bruketa T, Korolija D, et al. Lower incidence of hepatic metastases of colorectal cancer in patients with chronic liver diseases: meta-analysis. Hepatogastroenterology. 2013;60:1164–8.
4. Qi K, Qiu H, Sun D, et al. Impact of cirrhosis on the development of experimental hepatic metastases by B16F1 melanoma cells in C57BL/6 mice. Hepatology. 2004;40:1144–50.
5. Andreani V, Gatti G, Simonella L, et al. Activation of toll-like receptor 4 on tumor cells in vitro inhibits subsequent tumor growth in vivo. Cancer Res. 2007;67:10519–27.
6. Yan L, Cai Q, Xu Y. The ubiquitin-CXCR4 axis plays an important role in acute lung infection-enhanced lung tumor metastasis. Clin Cancer Res. 2013;19:4706–16.
7. Roy LD, Ghosh S, Pathangey LB, et al. Collagen induced arthritis increases secondary metastasis in MMTV-PyV MT mouse model of mammary cancer. BMC Cancer. 2011;11:365.
8. Das Roy L, Curry JM, Sahraei M, et al. Arthritis augments breast cancer metastasis: role of mast cells and SCF/c-Kit signaling. Breast Cancer Res. 2013;15:R32.
9. Zhang Y, Lamm WJ, Albert RK, et al. Influence of the route of allergen administration and genetic background on the murine allergic pulmonary response. Am J Respir Crit Care Med. 1997;155:661–9.
10. Lee JJ, Dimina D, Macias MP, et al. Defining a link with asthma in mice congenitally deficient in eosinophils. Science. 2004;305:1773–6.

11. Taranova AG, Maldonado 3rd D, Vachon CM, et al. Allergic pulmonary inflammation promotes the recruitment of circulating tumor cells to the lung. Cancer Res. 2008;68:8582–9.
12. Snyder JC, Reynolds SD, Hollingsworth JW, et al. Clara cells attenuate the inflammatory response through regulation of macrophage behavior. Am J Respir Cell Mol Biol. 2010;42:161–71.
13. Saha A, Lee YC, Zhang Z, et al. Lack of an endogenous anti-inflammatory protein in mice enhances colonization of B16F10 melanoma cells in the lungs. J Biol Chem. 2010;285:10822–31.
14. Minami T, Horiuchi K, Miura M, et al. Vascular endothelial growth factor- and thrombin-induced termination factor, Down syndrome critical region-1, attenuates endothelial cell proliferation and angiogenesis. J Biol Chem. 2004;279:50537–54.
15. Rothermel B, Vega RB, Yang J, et al. A protein encoded within the Down syndrome critical region is enriched in striated muscles and inhibits calcineurin signaling. J Biol Chem. 2000;275:8719–25.
16. Minami T, Miura M, Aird WC, et al. Thrombin-induced autoinhibitory factor, Down syndrome critical region-1, attenuates NFAT-dependent vascular cell adhesion molecule-1 expression and inflammation in the endothelium. J Biol Chem. 2006;281:20503–20.
17. Ryeom S, Baek KH, Rioth MJ, et al. Targeted deletion of the calcineurin inhibitor DSCR1 suppresses tumor growth. Cancer Cell. 2008;13:420–31.
18. Besse B, Lasserre SF, Compton P, et al. Bevacizumab safety in patients with central nervous system metastases. Clin Cancer Res. 2010;16:269–78.
19. Ferrara N, Carver-Moore K, Chen H, et al. Heterozygous embryonic lethality induced by targeted inactivation of the VEGF gene. Nature. 1996;380:439–42.
20. Minami T, Jiang S, Schadler K, et al. The calcineurin-NFAT-angiopoietin-2 signaling axis in lung endothelium is critical for the establishment of lung metastases. Cell Rep. 2013;4:709–23.
21. Robertson AL, Khairallah PA. Effects of angiotensin II and some analogues on vascular permeability in the rabbit. Circ Res. 1972;31:923–31.
22. De Ciuceis C, Amiri F, Brassard P, et al. Reduced vascular remodeling, endothelial dysfunction, and oxidative stress in resistance arteries of angiotensin II-infused macrophage colony-stimulating factor-deficient mice: evidence for a role in inflammation in angiotensin-induced vascular injury. Arterioscler Thromb Vasc Biol. 2005;25:2106–13.
23. Daugherty A, Rateri DL, Lu H, et al. Hypercholesterolemia stimulates angiotensin peptide synthesis and contributes to atherosclerosis through the AT1A receptor. Circulation. 2004;110:3849–57.
24. Ide N, Hirase T, Nishimoto-Hazuku A, et al. Angiotensin II increases expression of IP-10 and the renin-angiotensin system in endothelial cells. Hypertens Res. 2008;31:1257–67.
25. Sano H, Hosokawa K, Kidoya H, et al. Negative regulation of VEGF-induced vascular leakage by blockade of angiotensin II type 1 receptor. Arterioscler Thromb Vasc Biol. 2006;26:2673–80.
26. Imai Y, Kuba K, Rao S, et al. Angiotensin-converting enzyme 2 protects from severe acute lung failure. Nature. 2005;436:112–6.
27. Amano H, Ito Y, Ogawa F, et al. Angiotensin II type 1A receptor signaling facilitates tumor metastasis formation through P-selectin–mediated interaction of tumor cells with platelets and endothelial cells. Am J Pathol. 2013;182:553–64.
28. Ager EI, Neo J, Christophi C. The renin-angiotensin system and malignancy. Carcinogenesis. 2008;29:1675–84.
29. Kohlstedt K, Trouvain C, Namgaladze D, et al. Adipocyte-derived lipids increase angiotensin-converting enzyme (ACE) expression and modulate macrophage phenotype. Basic Res Cardiol. 2011;106:205–15.
30. Fujita M, Mason RJ, Cool C, et al. Pulmonary hypertension in TNF-alpha-overexpressing mice is associated with decreased VEGF gene expression. J Appl Physiol (1985). 2002;93:2162–70.

31. Jahr J, Grande PO. In vivo effects of tumor necrosis factor-alpha on capillary permeability and vascular tone in a skeletal muscle. Acta Anaesthesiol Scand. 1996;40:256–61.
32. Oliver PM, Fox JE, Kim R, et al. Hypertension, cardiac hypertrophy, and sudden death in mice lacking natriuretic peptide receptor A. Proc Natl Acad Sci U S A. 1997;94:14730–5.
33. Klinger JR, Tsai SW, Green S, et al. Atrial natriuretic peptide attenuates agonist-induced pulmonary edema in mice with targeted disruption of the gene for natriuretic peptide receptor-A. J Appl Physiol (1985). 2013;114:307–15.
34. Takashi Nojiri HH, Ishikane S, Kimura T, Kangawa K. ANP/GC-A signaling attenuates pulmonary metastasis of B16 melanoma enhanced by lipopolysaccharide or angiotensin-II. BMC Pharmacol Toxicol. 2013;14 Suppl 1:52.
35. Miyajima A, Kosaka T, Asano T, et al. Angiotensin II type I antagonist prevents pulmonary metastasis of murine renal cancer by inhibiting tumor angiogenesis. Cancer Res. 2002;62:4176–9.
36. Campbell WB, Falck JR. Arachidonic acid metabolites as endothelium-derived hyperpolarizing factors. Hypertension. 2007;49:590–6.
37. Panigrahy D, Edin ML, Lee CR, et al. Epoxyeicosanoids stimulate multiorgan metastasis and tumor dormancy escape in mice. J Clin Invest. 2012;122:178–91.
38. Koh YJ, Kang S, Lee HJ, et al. Bone marrow-derived circulating progenitor cells fail to transdifferentiate into adipocytes in adult adipose tissues in mice. J Clin Invest. 2007;117:3684–95.
39. Bannasch P, Klimek F, Mayer D. Early bioenergetic changes in hepatocarcinogenesis: preneoplastic phenotypes mimic responses to insulin and thyroid hormone. J Bioenerg Biomembr. 1997;29:303–13.
40. Metzger C, Bannasch P, Mayer D. Enhancement and phenotypic modulation of N-nitrosomorpholine-induced hepatocarcinogenesis by dehydroepiandrosterone. Cancer Lett. 1997;121:125–31.
41. Morimoto-Tomita M, Ohashi Y, Matsubara A, et al. Mouse colon carcinoma cells established for high incidence of experimental hepatic metastasis exhibit accelerated and anchorage-independent growth. Clin Exp Metastasis. 2005;22:513–21.
42. Hiratsuka S, Watanabe A, Sakurai Y, et al. The S100A8-serum amyloid A3-TLR4 paracrine cascade establishes a pre-metastatic phase. Nat Cell Biol. 2008;10:1349–55.
43. Deguchi A, Tomita T, Ohto U, et al. Eritoran inhibits S100A8-mediated TLR4/MD-2 activation and tumor growth by changing the immune microenvironment. Oncogene. 2016;35:1445–56.
44. Deguchi A, Tomita T, Omori T, et al. Serum amyloid A3 binds MD-2 to activate p38 and NF-kappaB pathways in a MyD88-dependent manner. J Immunol. 2013;191:1856–64.
45. Simard JC, Cesaro A, Chapeton-Montes J, et al. S100A8 and S100A9 induce cytokine expression and regulate the NLRP3 inflammasome via ROS-dependent activation of NF-kappaB(1.). PLoS One. 2013;8:e72138.
46. Hiratsuka S, Watanabe A, Aburatani H, et al. Tumour-mediated upregulation of chemoattractants and recruitment of myeloid cells predetermines lung metastasis. Nat Cell Biol. 2006;8:1369–75.
47. Anceriz N, Vandal K, Tessier PA. S100A9 mediates neutrophil adhesion to fibronectin through activation of beta2 integrins. Biochem Biophys Res Commun. 2007;354:84–9.
48. Martin MD, Carter KJ, Jean-Philippe SR, et al. Effect of ablation or inhibition of stromal matrix metalloproteinase-9 on lung metastasis in a breast cancer model is dependent on genetic background. Cancer Res. 2008;68:6251–9.
49. Wiechert L, Nemeth J, Pusterla T, et al. Hepatocyte-specific S100a8 and S100a9 transgene expression in mice causes Cxcl1 induction and systemic neutrophil enrichment. Cell Commun Signal. 2012;10:40.
50. Ieguchi K, Omori T, Komatsu A, et al. Ephrin-A1 expression induced by S100A8 is mediated by the toll-like receptor 4. Biochem Biophys Res Commun. 2013;440:623–9.

51. Larson J, Schomberg S, Schroeder W, et al. Endothelial EphA receptor stimulation increases lung vascular permeability. Am J Physiol Lung Cell Mol Physiol. 2008;295:L431–9.
52. Ieguchi K, Tomita T, Omori T, et al. ADAM12-cleaved ephrin-A1 contributes to lung metastasis. Oncogene. 2014;33:2179–90.
53. Yamazaki T, Masuda J, Omori T, et al. EphA1 interacts with integrin-linked kinase and regulates cell morphology and motility. J Cell Sci. 2009;122:243–55.
54. Tomita T, Sakurai Y, Ishibashi S, et al. Imbalance of Clara cell-mediated homeostatic inflammation is involved in lung metastasis. Oncogene. 2011;30:3429–39.
55. Bessede A, Gargaro M, Pallotta MT, et al. Aryl hydrocarbon receptor control of a disease tolerance defence pathway. Nature. 2014;511:184–90.
56. Patel RD, Murray IA, Flaveny CA, et al. Ah receptor represses acute-phase response gene expression without binding to its cognate response element. Lab Invest. 2009;89:695–707.
57. Qian BZ, Li J, Zhang H, et al. CCL2 recruits inflammatory monocytes to facilitate breast-tumour metastasis. Nature. 2011;475:222–5.
58. Apetoh L, Ghiringhelli F, Tesniere A, et al. Toll-like receptor 4-dependent contribution of the immune system to anticancer chemotherapy and radiotherapy. Nat Med. 2007;13:1050–9.
59. von Bernuth H, Picard C, Jin Z, et al. Pyogenic bacterial infections in humans with MyD88 deficiency. Science. 2008;321:691–6.
60. Ngo VN, Young RM, Schmitz R, et al. Oncogenically active MYD88 mutations in human lymphoma. Nature. 2011;470:115–9.
61. St John AL, Abraham SN. Salmonella disrupts lymph node architecture by TLR4-mediated suppression of homeostatic chemokines. Nat Med. 2009;15:1259–65.
62. Yamada M, Kubo H, Kobayashi S, et al. Bone marrow-derived progenitor cells are important for lung repair after lipopolysaccharide-induced lung injury. J Immunol. 2004;172:1266–72.
63. Haricharan S, Brown P. TLR4 has a TP53-dependent dual role in regulating breast cancer cell growth. Proc Natl Acad Sci U S A. 2015;112:E3216–25.
64. Andonegui G, Bonder CS, Green F, et al. Endothelium-derived toll-like receptor-4 is the key molecule in LPS-induced neutrophil sequestration into lungs. J Clin Invest. 2003;111:1011–20.
65. Bresnick AR, Weber DJ, Zimmer DB. S100 proteins in cancer. Nat Rev Cancer. 2015;15:96–109.
66. Manitz MP, Horst B, Seeliger S, et al. Loss of S100A9 (MRP14) results in reduced interleukin-8-induced CD11b surface expression, a polarized microfilament system, and diminished responsiveness to chemoattractants in vitro. Mol Cell Biol. 2003;23:1034–43.
67. Leanderson T, Liberg D, Ivars F. S100A9 as a pharmacological target molecule in inflammation and cancer. Endocr Metab Immune Disord Drug Targets. 2015;15:97–104.
68. Odink K, Cerletti N, Bruggen J, et al. Two calcium-binding proteins in infiltrate macrophages of rheumatoid arthritis. Nature. 1987;330:80–2.
69. Yanamandra K, Alexeyev O, Zamotin V, et al. Amyloid formation by the pro-inflammatory S100A8/A9 proteins in the ageing prostate. PLoS One. 2009;4:e5562.
70. Vogl T, Leukert N, Barczyk K, et al. Biophysical characterization of S100A8 and S100A9 in the absence and presence of bivalent cations. Biochim Biophys Acta. 2006;1763:1298–306.
71. Tyden H, Lood C, Gullstrand B, et al. Increased serum levels of S100A8/A9 and S100A12 are associated with cardiovascular disease in patients with inactive systemic lupus erythematosus. Rheumatology (Oxford). 2013;52:2048–55.
72. Foell D, Wittkowski H, Ren Z, et al. Phagocyte-specific S100 proteins are released from affected mucosa and promote immune responses during inflammatory bowel disease. J Pathol. 2008;216:183–92.
73. Keller M, Ruegg A, Werner S, et al. Active caspase-1 is a regulator of unconventional protein secretion. Cell. 2008;132:818–31.
74. Ghiringhelli F, Apetoh L, Tesniere A, et al. Activation of the NLRP3 inflammasome in dendritic cells induces IL-1beta-dependent adaptive immunity against tumors. Nat Med. 2009;15:1170–8.

75. Grebhardt S, Veltkamp C, Strobel P, et al. Hypoxia and HIF-1 increase S100A8 and S100A9 expression in prostate cancer. Int J Cancer. 2012;131:2785–94.
76. Hsu K, Passey RJ, Endoh Y, et al. Regulation of S100A8 by glucocorticoids. J Immunol. 2005;174:2318–26.
77. Spijkers-Hagelstein JA, Schneider P, Hulleman E, et al. Elevated S100A8/S100A9 expression causes glucocorticoid resistance in MLL-rearranged infant acute lymphoblastic leukemia. Leukemia. 2012;26:1255–65.
78. Vogl T, Tenbrock K, Ludwig S, et al. Mrp8 and Mrp14 are endogenous activators of toll-like receptor 4, promoting lethal, endotoxin-induced shock. Nat Med. 2007;13:1042–9.
79. Turovskaya O, Foell D, Sinha P, et al. RAGE, carboxylated glycans and S100A8/A9 play essential roles in colitis-associated carcinogenesis. Carcinogenesis. 2008;29:2035–43.
80. Kislinger T, Fu C, Huber B, et al. N(epsilon)-(carboxymethyl)lysine adducts of proteins are ligands for receptor for advanced glycation end products that activate cell signaling pathways and modulate gene expression. J Biol Chem. 1999;274:31740–9.
81. Xie J, Burz DS, He W, et al. Hexameric calgranulin C (S100A12) binds to the receptor for advanced glycated end products (RAGE) using symmetric hydrophobic target-binding patches. J Biol Chem. 2007;282:4218–31.
82. Hofmann MA, Drury S, Fu C, et al. RAGE mediates a novel proinflammatory axis: a central cell surface receptor for S100/calgranulin polypeptides. Cell. 1999;97:889–901.
83. Leclerc E, Fritz G, Weibel M, et al. S100B and S100A6 differentially modulate cell survival by interacting with distinct RAGE (receptor for advanced glycation end products) immunoglobulin domains. J Biol Chem. 2007;282:31317–31.
84. Chen H, Xu C, Jin Q, et al. S100 protein family in human cancer. Am J Cancer Res. 2014;4:89–115.
85. Zibert JR, Skov L, Thyssen JP, et al. Significance of the S100A4 protein in psoriasis. J Invest Dermatol. 2010;130:150–60.
86. Gebhardt C, Riehl A, Durchdewald M, et al. RAGE signaling sustains inflammation and promotes tumor development. J Exp Med. 2008;205:275–85.
87. Bjork P, Bjork A, Vogl T, et al. Identification of human S100A9 as a novel target for treatment of autoimmune disease via binding to quinoline-3-carboxamides. PLoS Biol. 2009;7:e97.
88. Hibino T, Sakaguchi M, Miyamoto S, et al. S100A9 is a novel ligand of EMMPRIN that promotes melanoma metastasis. Cancer Res. 2013;73:172–83.
89. Arnold V, Cummings JS, Moreno-Nieves UY, et al. S100A9 protein is a novel ligand for the CD85j receptor and its interaction is implicated in the control of HIV-1 replication by NK cells. Retrovirology. 2013;10:122.
90. Gilchrist M, Thorsson V, Li B, et al. Systems biology approaches identify ATF3 as a negative regulator of Toll-like receptor 4. Nature. 2006;441:173–8.
91. Boespflug ND, Kumar S, McAlees JW, et al. ATF3 is a novel regulator of mouse neutrophil migration. Blood. 2014;123:2084–93.
92. Gilchrist M, Henderson Jr WR, Clark AE, et al. Activating transcription factor 3 is a negative regulator of allergic pulmonary inflammation. J Exp Med. 2008;205:2349–57.
93. Wolford CC, McConoughey SJ, Jalgaonkar SP, et al. Transcription factor ATF3 links host adaptive response to breast cancer metastasis. J Clin Invest. 2013;123:2893–906.
94. Han C, Jin J, Xu S, et al. Integrin CD11b negatively regulates TLR-triggered inflammatory responses by activating Syk and promoting degradation of MyD88 and TRIF via Cbl-b. Nat Immunol. 2010;11:734–42.
95. Kang YJ, Kusler B, Otsuka M, et al. Calcineurin negatively regulates TLR-mediated activation pathways. J Immunol. 2007;179:4598–607.
96. Androulidaki A, Iliopoulos D, Arranz A, et al. The kinase Akt1 controls macrophage response to lipopolysaccharide by regulating microRNAs. Immunity. 2009;31:220–31.
97. Kalyana-Sundaram S, Kumar-Sinha C, Shankar S, et al. Expressed pseudogenes in the transcriptional landscape of human cancers. Cell. 2012;149:1622–34.

98. Tomita T, Ieguchi K, Sawamura T, et al. Human serum amyloid A3 (SAA3) protein, expressed as a fusion protein with SAA2, binds the oxidized low density lipoprotein receptor. PLoS One. 2015;10:e0118835.
99. Han CY, Subramanian S, Chan CK, et al. Adipocyte-derived serum amyloid A3 and hyaluronan play a role in monocyte recruitment and adhesion. Diabetes. 2007;56:2260–73.
100. Reigstad CS, Lunden GO, Felin J, et al. Regulation of serum amyloid A3 (SAA3) in mouse colonic epithelium and adipose tissue by the intestinal microbiota. PLoS One. 2009;4:e5842.
101. Yan HH, Pickup M, Pang Y, et al. Gr-1+CD11b+ myeloid cells tip the balance of immune protection to tumor promotion in the premetastatic lung. Cancer Res. 2010;70:6139–49.
102. van Hogerlinden M, Rozell BL, Ahrlund-Richter L, et al. Squamous cell carcinomas and increased apoptosis in skin with inhibited Rel/nuclear factor-kappaB signaling. Cancer Res. 1999;59:3299–303.
103. Lind MH, Rozell B, Wallin RP, et al. Tumor necrosis factor receptor 1-mediated signaling is required for skin cancer development induced by NF-kappaB inhibition. Proc Natl Acad Sci U S A. 2004;101:4972–7.
104. Ulvmar MH, Sur I, Memet S, et al. Timed NF-kappaB inhibition in skin reveals dual independent effects on development of HED/EDA and chronic inflammation. J Invest Dermatol. 2009;129:2584–93.
105. Asagiri M, Takayanagi H. The molecular understanding of osteoclast differentiation. Bone. 2007;40:251–64.
106. Jones DH, Nakashima T, Sanchez OH, et al. Regulation of cancer cell migration and bone metastasis by RANKL. Nature. 2006;440:692–6.
107. Mikami S, Katsube K, Oya M, et al. Increased RANKL expression is related to tumour migration and metastasis of renal cell carcinomas. J Pathol. 2009;218:530–9.
108. Kikuchi T, Matsuguchi T, Tsuboi N, et al. Gene expression of osteoclast differentiation factor is induced by lipopolysaccharide in mouse osteoblasts via toll-like receptors. J Immunol. 2001;166:3574–9.
109. Chakravarti A, Raquil MA, Tessier P, et al. Surface RANKL of toll-like receptor 4-stimulated human neutrophils activates osteoclastic bone resorption. Blood. 2009;114:1633–44.
110. Inada M, Takita M, Yokoyama S, et al. Direct melanoma cell contact induces stromal cell autocrine prostaglandin E2-EP4 receptor signaling that drives tumor growth, angiogenesis and metastasis. J Biol Chem. 2015;290:29781–93.
111. Liao Y, Day KH, Damon DN, et al. Endothelial cell-specific knockout of connexin 43 causes hypotension and bradycardia in mice. Proc Natl Acad Sci U S A. 2001;98:9989–94.
112. Li K, Yao J, Shi L, et al. Reciprocal regulation between proinflammatory cytokine-induced inducible NO synthase (iNOS) and connexin43 in bladder smooth muscle cells. J Biol Chem. 2011;286:41552–62.
113. Stoletov K, Strnadel J, Zardouzian E, et al. Role of connexins in metastatic breast cancer and melanoma brain colonization. J Cell Sci. 2013;126:904–13.
114. Wang L, Chang EW, Wong SC, et al. Increased myeloid-derived suppressor cells in gastric cancer correlate with cancer stage and plasma S100A8/A9 proinflammatory proteins. J Immunol. 2013;190:794–804.
115. Matzinger P. Tolerance, danger, and the extended family. Annu Rev Immunol. 1994;12:991–1045.
116. Pradeu T, Cooper EL. The danger theory: 20 years later. Front Immunol. 2012;3:287.